

XAI and Statistical Analysis for Reliable Intrusion Detection in the UVIDS-2025 Dataset: From Tree to Hybrid and Tabular DNN Ensembles

Iakovos-Christos Zarkadis
University of Piraeus
Athens, Greece
iakovos.zarkadis@gmail.com

Christos Douligeris
Dept. of Informatics
University of Piraeus
Piraeus, Greece
cdoulig@unipi.gr

Abstract—During the last few years, the term Mechanistic Interpretability, a specific area, under the umbrella of explainable artificial intelligence (XAI), has been introduced, to explain the decisions made by complex machine learning (ML) models in critical systems like UAV intrusion detection systems (UVIDS). In this paper, we apply best-practices for data pre-processing and examine a wide range of tree-ensembles, deep neural networks, hybrid stacking models and the latest ensemble neural networks to detect intrusions in UAV, with stratified 10-fold cross validation. With our top-performing model, XGBoost, we proceed to Shapley Additive explanations (SHAP), to analyze the global and local feature importances and understand which features, each attack targets, to mimic normal traffic and where the misclassifications occur. Furthermore a distribution analysis follows, by visually comparing violin plots and the curves of kernel density estimations. With the Westfall-Young permutation test for multiple comparisons, the Bandwidth optimization of the KDEs and the selection of Jensen-Shannon Distance for the test, we discover the true causes of false predictions, observed in Wormhole and Blackhole attacks in UVIDS-2025. The findings provide robust, reliable and explainable models for UAV intrusion detection, along with statistical insights, which capture and clarify the masked nature of the attacks, regarding the challenge of Density Support Intersection, between these attacks, in this dataset.

Index Terms—Machine learning (ML), explainable artificial intelligence (XAI), unmanned aerial vehicle network intrusion detection systems (UVIDS), deep neural networks (DNN), Shapley Additive explanation (SHAP).

I. INTRODUCTION

Explainable techniques have gained recently everyone’s attention, due to their diversity and wide area of application. UAV intrusion detection, has gathered the attention of the research society for its many applications and dangers, that may occur in IoT networks in combination with the rise of 6G networks and their AI integration [2], [13], [19]. XAI methods, such as SHAP, LIME, Grad-CAM have been implemented in research papers, regarding UAV and IoT intrusion detection [5], [8], [11], [12], [14]. Methods like these, have been applied, for a great variety of algorithmic families, such as, Tree-based models, like Decision and Extra trees [1], [20], ensemble models, like XGBoost, LightGBM [9], [11], [12], neural networks and deep learning, like MLP, RNN, CNN,

LSTM [24]. Due to the critical role of IoT networks, many frameworks have been designed, that combine deep, ensemble and federated learning to enhance intrusion detection [3], [23]. Modern frameworks direct their focus in explainability of predictions, of different modalities and models [5], [14], [21], [26], [28], [29]. Other newer frameworks focus on explainable Agentic AI [27]. Our focus in this paper, is first, to apply best pre-processing practices to ensure high data-quality, to have reliable, faithful and explainable results that provide deep insight about our data’s true nature. We apply a great variety of, well known, state-of-the-art tree-ensembles, like XGBoost [20], LightGBM, Histogram-Based Gradient Boosting, Random Forest, hybrid ensembles that combine linear, tree and bayesian models [10], deep neural networks, like RealMLP and deep neural network ensembles, like Ensemble-RealMLP, from some of the latest frameworks, such as AutoGluon and PyTabKit, designed specifically for tabular data [4], [15]. After we select our best classifier, XGBoost, we proceed to explainable techniques, with SHAP [22], like local and global feature importances, in order to analyze how his internal mechanism makes predictions and optimize his decisions. Next we examine the shape of our data, through Box-Plots, per attack, but also their densities and distribution shapes, with violin and Kernel Density Estimations [25], to better understand their univariate nature, along with the challenges that they bring up. Clear evidences are provided, for specific true and false predictions, of selected observations. In the end to really understand and explain the major issue with this dataset, Density Support Intersection, between Blackhole and Wormhole attacks, in most of their feature space, we apply a robust statistical non-parametric Westfall-Young test, for a total of $B = 1000$ permutations [7], [16], [17], with bandwidth-optimized KDEs. For this test we calculate Family-Wise Error Rate adjusted $p - values$, to ensure statistical significance, for our multiple comparisons, thus avoiding the Bonferroni correction issues. The statistical function of the test is the Max-Statistic of the Jensen-Shannon distances obtained from the permutations. The chosen procedure provides reliable examination and detection of Support Intersection scenarios, for masked attacks in UAV networks. This work is organized in

two sections. In the first we present the pre-processing steps and the UAV intrusion detection results. In the second we apply SHAP analysis to provide global and local explainability and the non-parametric test, with the KDEs, to provide probabilistic evidence of the major challenge of Density Support Intersection, faced in UVAIDS-2025.

II. MACHINE LEARNING-BASED UVAIDS METHODOLOGY

A. Data Collection

For all the results that will be presented in the next sections we used the UVAIDS-2025 dataset, a recently uploaded tabular dataset for unmanned aerial vehicle network intrusion detection, which contains around 120,000 observations, 22 features and the target variable [12], [18]. The target variable has four types of attacks (Sybil, Blackhole, Wormhole, Flooding) and one for the normal traffic. The dataset is not heavily unbalanced, so there is no need for synthetic sampling techniques.

B. Data Pre-Processing

The pre-processing procedure started by omitting the duplicate values, then removing the redundant feature "Protocol", since the only protocol, which exists is "UDP". In addition, we removed the indexing variable, "FlowID", since it is not a real variable, due to the bias and disruption, which introduces, in Tab. IV of [12], as seen by the feature importances. After that followed, the label-encoding of the target variable. Furthermore, we performed dummy encoding for the source and destination ports and frequency encoding for the destination and source IP address. Next the data were splitted into 80/20 train/test, in a stratified way, with respect to the target variable, the label. Then we engineered a few features with power and reciprocal transformations. After discovering outliers, with IQR and Box-Plots the Robust scaler was selected.

To conclude to the most important features, we used Recursive Feature Elimination with a Random Forest and obtained the feature importance plot in Fig. 1. The ones selected from RFE, where those with a percentage of contribution higher than 2.5%.

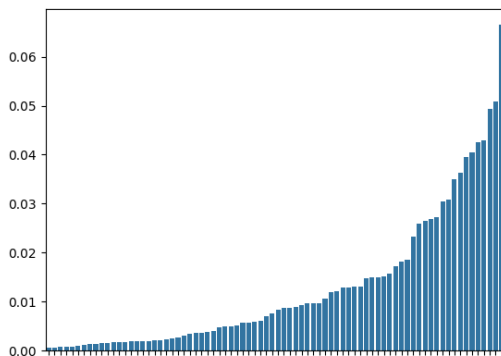
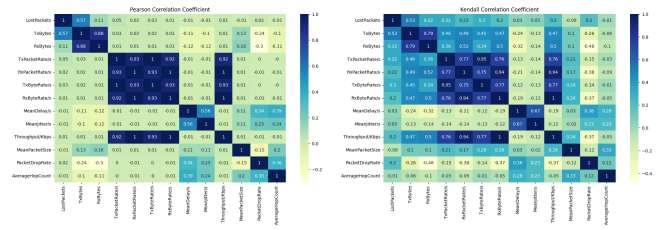


Fig. 1: RFE for the Random Forest

From the feature selection, the ones selected can be seen in Fig. 2, where the Pearson and Kendall correlation heatmaps are plotted, for the numerical features.

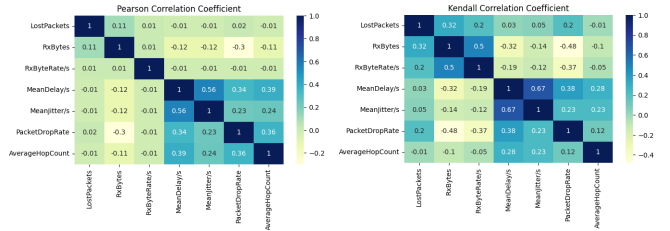


(a) Pearson

(b) Kendall

Fig. 2: Correlation Coefficients after Feature Selection

From these we observe some high correlations, that need to be removed for the SHAP analysis, to avoid misleading results. An example is the use of the variables "TxByteRate/s", "TxPacketRate/s", "RxByteRate/s" and "RxPacketRate/s", in [12], which share a non-linear correlation > 0.7 , that raises the danger of multi-collinearity, for false interpretations. We consider a threshold of ≥ 0.7 and remove the ones that exceed it, thus leading us to the below correlation heatmaps in Fig. 3.



(a) Pearson

(b) Kendall

Fig. 3: Correlation Coefficients after Dropping Correlated Features for SHAP

The remaining features can be seen below in Tab. I

TABLE I: Explainable Intrusion Detection Selected Features

<i>Selected Features</i>
LostPackets, RxBytes, RxByteRate/s, MeanDelay/s, MeanJitter/s, PacketDropRate, AverageHopCount, DstPort654

C. Intrusion Detection

For the classification of the tabular data, our experiments are concentrated in tree-ensembles, like bagging and boosting, deep neural networks, stacking ensembles of deep neural networks and hybrid stacking ensemble models that combine trees, ensembles and linear models, with Gaussian Naive Bayes. The baseline models are Logistic Regression and an SVM. The tree ensembles are XGBoost, XGBoost with Random Forest, Random Forest, LightGBM, Extra-Trees, Gradient Boosting, Histogram-Based Gradient Boosting, Decision-Tree-Based AdaBoost, Decision-Tree-Based Bagging. The first hybrid stacking model (Stacking-1) that we chose contains a Decision Tree, a Histogram-Based Gradient Boosting and a Gaussian Naive Bayes as base estimators and Ridge as the

final estimator. The second hybrid model (Stacking-2) contains a Decision Tree, a Logistic Regression and a Gaussian Naive Bayes as base estimators and Ridge as the final estimator. The neural networks are MPL and RealMLP. Also the following stacking ensemble versions of deep neural networks RealMLP, NNFastAiTabular and NN-Torch, from the AutoGluon and PyTabKit libraries have been selected [4], [15]. Grid-search, along with stratified 10-fold cross validation was combined for hyperparameter tuning. After selecting the optimal hyperparameters, each of the pre-mentioned models was trained with stratified 10-fold cross validation, with probability calibration, while holding a 4% value range threshold for considering a model stable per evaluation metric.

The evaluation metrics, with which we evaluated the performance of each algorithm are F1, Precision, Recall, and Roc-Auc. From the metric results, in Tab. II and Tab. III, we observe that all tree-ensembles achieve score over 92%, which explains their superiority, with XGBoost being the best-performing of its type. Furthermore, we observe very good to excellent performances, from the neural networks and to be more specific, of RealMLP. The ensemble neural networks have good to outstanding results, with the Ensemble versions of RealMLP and NN-Torch being the ones that stand out. Regarding the two baseline models, Logistic Regression struggles, while the SVM has a nearly-acceptable performance.

TABLE II: Train/Test Precision and Recall Results (%)

Model	Train/Test-Precision	Train/Test-Recall
XGBoost	96.60/95.17	96.50/95.04
XGBoost-RF	95.58/94.56	95.49/94.44
Random Forest	95.75/94.17	95.68/94.09
LightGBM	95.19/94.27	94.95/94.01
Extra-Trees	92.90/91.20	92.52/90.80
Gradient Boosting	92.29/91.71	92.19/91.62
HB-Gradient Boosting	92.77/92.31	92.64/92.17
AdaBoost(DT)	95.91/94.85	95.18/93.93
Bagging (DT)	93.51/92.71	93.43/92.65
Stacking-1	94.88/94.05	94.78/93.95
Stacking-2	66.15/65.85	65.36/65.23
MLP	91.20/90.70	91.13/90.65
RealMLP	95.00/94.49	94.80/94.28
Ensemble-RealMLP	94.26/93.71	94.07/93.51
Ensemble-NNFastAiTab	86.63/86.30	85.69/85.34
Ensemble-NN-Torch	94.14/93.72	93.85/93.43
SGD-SVM	74.46/74.21	72.73/72.40
Logistic Regression	49.20/49.50	48.74/48.90

To highlight the value of reliable training through stratified cross-validation we present the calibrated cross-validation results, of RealMLP, for precision and recall in Fig. 4, where we observe stability, within the 4% value range.

The confusion matrices for the training and testing set, for XGBoost, can be seen below in Fig. 5. It is worth to mention that, both for in-sample and out-of-sample data, only a few Wormhole attacks trick the XGBoost, to misclassify them as Normal traffic. We can also see how XGBoost confuses some Blackhole attacks for Wormhole attacks and vice versa. All of these findings will be presented and justified in the following section.

TABLE III: Train/Test F1 and Roc-Auc Results (%)

Model	Train/Test-F1	Train/Test-Roc-Auc
XGBoost	96.50/95.04	97.77/96.85
XGBoost-RF	95.49/94.45	97.14/96.48
Random Forest	95.68/94.09	97.26/96.26
LightGBM	94.95/94.02	96.80/96.21
Extra-Trees	92.56/90.84	95.27/94.18
Gradient Boosting	92.19/91.62	95.08/94.72
HB-Gradient Boosting	92.65/92.19	95.36/95.07
AdaBoost(DT)	95.15/93.92	96.93/96.15
Bagging (DT)	93.44/92.65	95.86/95.37
Stacking-1	94.79/93.96	94.78/93.95
Stacking-2	62.77/62.68	78.18/78.10
MLP	91.15/90.66	94.40/94.09
RealMLP	94.80/94.28	96.71/96.38
Ensemble-RealMLP	94.06/93.51	96.24/95.89
Ensemble-NNFastAiTab	85.90/85.56	90.98/90.76
Ensemble-NN-Torch	93.87/93.44	96.12/95.86
SGD-SVM	73.19/72.87	82.82/82.61
Logistic Regression	46.93/47.13	67.80/67.89

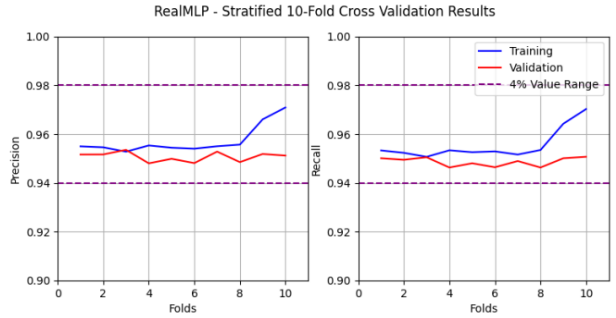


Fig. 4: RealMLP Stratified 10-Fold CV.

III. EXPLAINABILITY

To gain actual and trustworthy insight from our trained models, we will perform SHAP analysis, for our best model, XGBoost. Our Methodology starts by examining global and local explanations. Then we move to distribution analysis with violin plots, kernel density estimations and statistical divergence computation. Last but not least, we target the features that cause misclassifications, to get real insight about why and where our best model gets tricked. For most of our analysis, we utilized the SHAPASH framework.

A. Global/Local Explanations

To understand the overall decision-making process of our model, XGBoost, we begin with global feature importances.

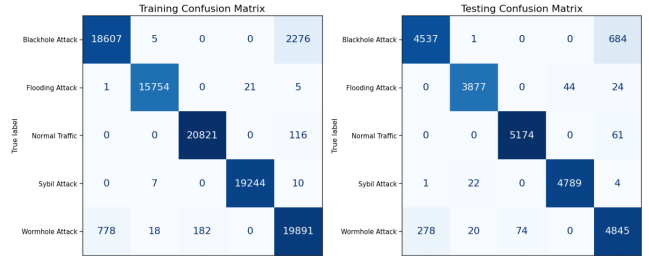


Fig. 5: XGBoost Confusion Matrices

In Fig. 6 we observe those, per label and it is clear that the features with the highest impact for most of the classes are "PacketDropRate", "RxByteRate/s", "RxBytes" and "DstPort654". From the same figure, we can understand, in-general, how each attack prioritizes the variables, that play a major role for a packet to be labeled as normal traffic (importance ≥ 0.1). Furthermore to compare XGBoost's efficiency with MLP, we present in Fig. 7 the global feature importances per label. From this we notice how the algorithm's decision are based obviously on the features mentioned above, but also at a higher percentage in the variables "MeanDelay/s", "AverageHopCount" and "MeanJitter/s", which causes the larger percentage of misclassifications.

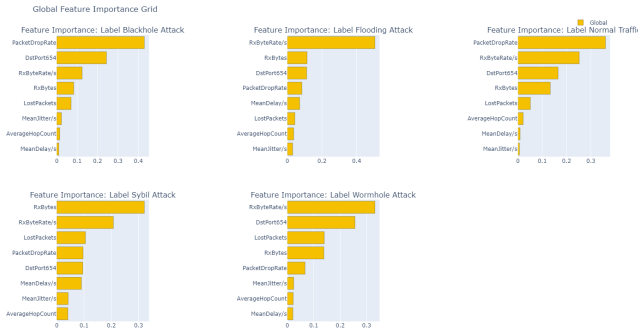


Fig. 6: XGBoost Global Feature Importances per Label.

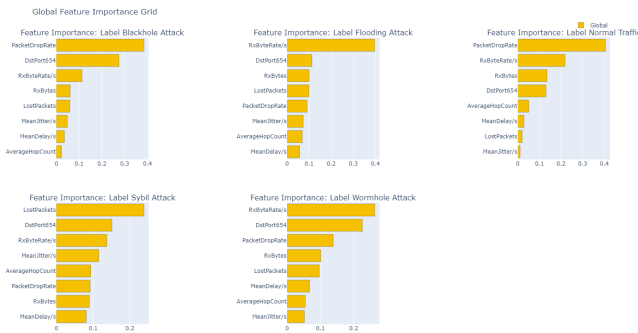


Fig. 7: MLP Global Feature Importances per Label.

Moving to local explanations, as seen in Fig. 8, for our best model, we see, if we look closely, how the importances in the variables "MeanDelay/s", "AverageHopCount" and "MeanJitter/s" have raised compared to the global ones. These findings prove that, misclassifications may occur, due to the fact that certain features, per label always, have larger percentage of contribution to some individual observations. As we can see from Fig. 9, for MLP, the local feature importances to these three pre-mentioned variables, is even larger and more specifically in Sybil and Wormhole attacks. That justifies the lower performance of MLP, compared to XGBoost.

B. Shape Explanations

Below in Fig. 10 the Box-Plots per label can be seen and we notice the large number of outliers that exist in some variables. It is significant to mention, how similar is the dispersion of the

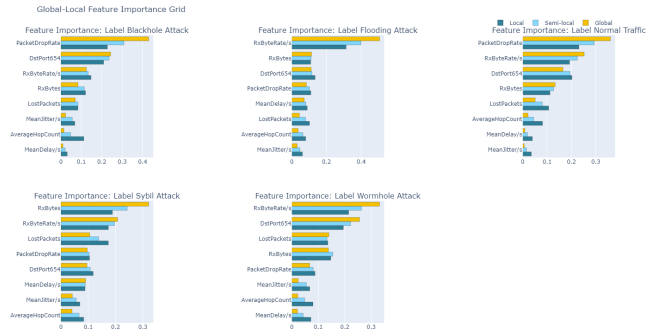


Fig. 8: XGBoost Global, Local, Semi-Local Feature Importance per Label.

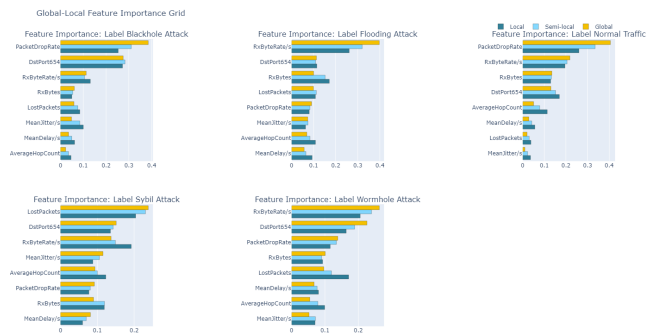


Fig. 9: MLP Global, Local, Semi-Local Feature Importances per Label.

outliers, for the features "MeanDelay/s", "AverageHopCount" and "MeanJitter/s" in the Wormhole and Blackhole attacks, the ones, in which the misclassifications occur in XGBoost, between these two classes. Their similarities, in terms of density, skewness and center of mass, is highlighted, with the aid of violin plots in Fig. 11. This reveals that, our best model has room for improvement, in similar heavy outlier tails, between globally less important features. Such misclassification scenarios, for the dilemma of Blackhole or Wormhole, are avoided when the variable "PacketDropRate" obtains high values. Otherwise with values close to the median the model becomes hesitant. False predictions, between these two classes, when the model exists in ambiguity, due to the pre-mentioned reasons, can obviously arise, from the outliers of "DstPort654", as seen in the Wormhole attack.

An easy way to analyze the shapes of our variables, along with their skewness, are the violin plots as seen in Fig. 11. For each violin plot, the positive values push the probability of prediction, higher, towards the label, to which the plot corresponds to. The negative values lower the probability. In some features we see extremely long right tails in most of the classes and in combination with the center of mass being concentrated near zero, in the y-axis, we can understand that extreme events, have very high impact on the model's decision. For example in the Flooding attack, all variables, but "RxByteRate/s", have long tails in their violin plots and wide center of mass around zero, meaning that rare observations

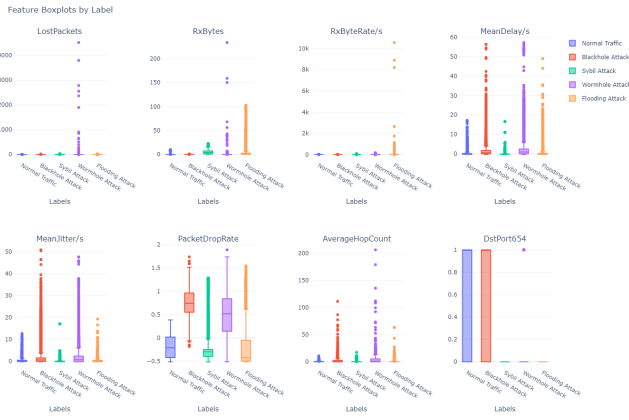


Fig. 10: Feature Box-Plots per Label.

make the difference in XGBoost’s decisions. For the same attack, it is also interesting, that in the variable ”RxByteRate/s”, we have observations that aid both in the increase and decrease of the probability, but then it’s heavy right tail slightly thickens at the end, which indicates a second peak in it’s probability density function. The same we observe in the Wormhole attack for variable ”RxByteRate/s”. The data-points located in that spot, rule the model’s decisions, towards labeling a packet as Flooding. Furthermore by comparing the violins, in features ”MeanDelay/s”, ”AverageHopCount” and ”MeanJitter/s”, between Blackhole and Wormhole attacks, we notice their extreme shape similarity, in terms of density, thickness and long right tails, which supports the previous findings on the global and local explanations. This tells us that these features probably confuse the model, for these classes, because of their high similarity. About the two peaks mentioned above, we detect this phenomenon in other features and more specifically in labels Flooding, Sybil, Blackhole attack, but also in Normal traffic. These are indications of multi-modal distributions. To conclude with the violin plots, our best model is capable of identifying a large amount of rare events and make clever decisions, without being tricked by the high variance of our data and their multi-modal densities, in most cases.

We applied Kernel Density Estimation, with Gaussian kernel and Scott bandwidth, as a visualization method to get a first general idea [25]. The visualizations can be seen in Fig. 12 and Fig. 13. From those, we clarify long and heavy tails, as well as bimodal distributions. Additionally, we highlight, how similar some distributions are, in features like ”LostPackets”, ”RxByteRate/s” and ”RxBytes”.

C. Uncertainty in Blackhole and Wormhole Attacks

To be more specific in our analysis, in Fig. 14, we see the local explanation for the 7th observation of our training dataset, which focuses on the Blackhole-Wormhole dilemma. This observation is a Wormhole attack, but is predicted as Blackhole. The variables ”AverageHopCount”, ”MeanDelay/s” and ”MeanJitter/s”, all share high values, which is observed in both classes and it doesn’t really help. The negative values



Fig. 11: XGBoost Feature Violin Plots per Label.

observed in ”LostPackets”, stand for values below and close to the median of the distribution, after the transformation with the Robust scaler, which are indications of Blackhole attack. This because from both the Box-Plots and Violin plots in Fig. 10 and Fig. 11, respectively, we see longer tails in this variable, for Wormhole attacks. The only clear indications for it, to be labeled as Wormhole is the destination port with value 0. From the differentiator variable, ”PacketDropRates”, we see a value of 0.63, which means it is located ahead of the median, a clue that supports the Blackhole scenario, as seen by the right heavy tail in the Box-Plot in Fig. 10.

In Fig. 15, we highlight, how a solid decision looks like for a Blackhole attack. First the variable ”PacketDropRate”, has a high value, ahead of the median, leaning in favor of Blackhole. From the value 1 in ”DstPort654” we observe the same, as well as from the ”RxBytes”, because it is located close to the median. The only suspicion that could probably rise is the value of ”LostPackets”, because such high values are observed in the Wormhole Attacks, as it can be verified from Fig. 10.



Fig. 12: KDEs per Label

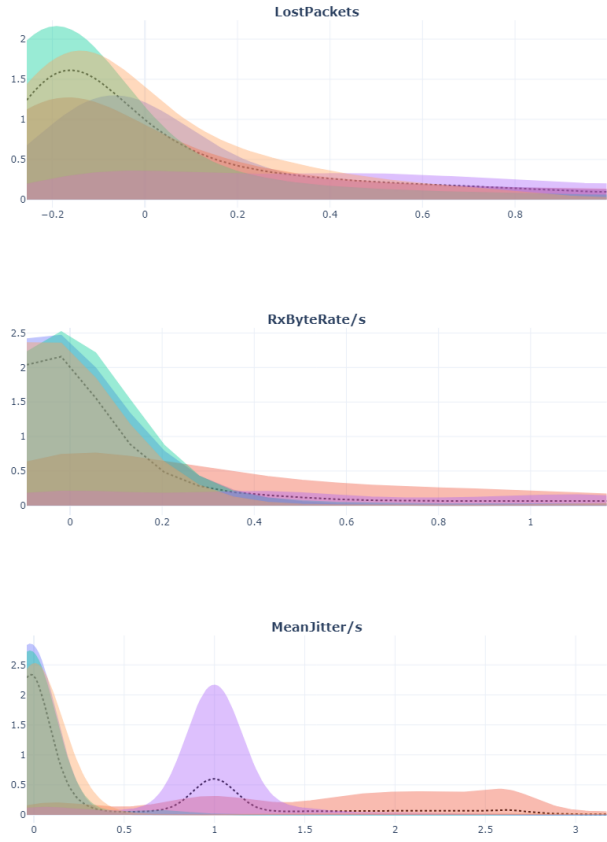


Fig. 13: KDEs per Label

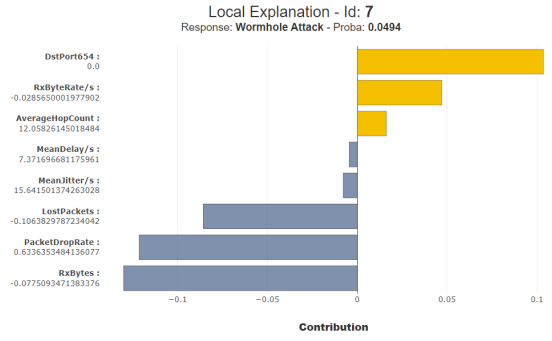


Fig. 14: Local Explanation for the 7th observation

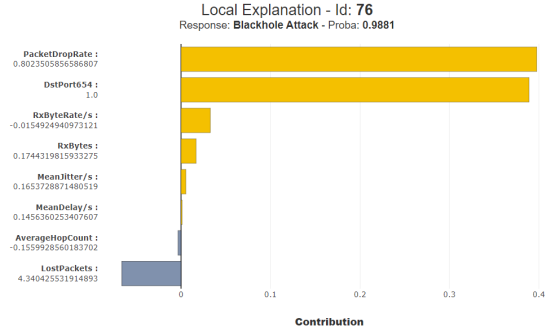


Fig. 15: Local Explanation for the 76th observation

D. Density Estimation and Westfall-Young Permutation Test

To gain deeper statistical insights about our model's decision's we will perform the Westfall-Young Permutation Test, for a total of 1000 permutations [16], [17] and Kernel Density Estimation with Bandwidth optimization [25]. Due to the misclassifications that occurred, in the confusion matrix, between the classes Blackhole and Wormhole, we must search for the cause. Let $P_{i,k}$ be the distribution of the k -th class, for the i -th feature. For each of our continuous features, $i = 1, 2, \dots, p$, with $p = 7$ and our two selected classes, $k = V, W$, we can formulate the hypothesis seen in "(1)", which addresses the equality of two density estimations. In our Max-Statistic test we have the following hypothesis, as seen in "(2)", hence it is called multiple testing [16], [17], for a total of i features and two classes W and V :

$$H_0 : P_{i,V} = P_{i,W} \text{ against } H_1 : P_{i,V} \neq P_{i,W} \quad (1)$$

$$H_0 : P_{i,V} = P_{i,W}, i \in \{1, 2, \dots, 7\} \text{ against } H_1 : P_{i,V} \neq P_{i,W}, \exists i \in \{1, 2, \dots, 7\} \quad (2)$$

Because we will address only two categories, consider $P_{j,W} = Q_i$. Both $P_i(x), Q_i(x)$ are estimated with Kernel Density Estimation, with Gaussian kernel and an embedded cross validation, for optimal bandwidth selection [25]. For this procedure, we select as a test statistic the Jensen-Shannon distance (Square Root of Jensen-Shannon divergence):

$$T_i = JS_{Dist}(P_i, Q_i) = \sqrt{JS_{Div}(P_i, Q_i)} = \sqrt{\frac{1}{2}D_{KL}(P_i, M_i) + \frac{1}{2}D_{KL}(Q_i, M_i)}, \text{ with}$$

$$D_{KL}(P_i, M_i) = \sum_{x \in \{x_B, x_W\}} P_i(x) \log_2 \left(\frac{P_i(x)}{M_i(x)} \right), \quad (3)$$

$$M_i(x) = \frac{1}{2}(P_i(x) + Q_i(x)), \quad i = 1, 2, \dots, p$$

The Max-Statistic for the b -th permutation is:

$$T_b^{JSD} = \max\{T_{1b}, T_{2b}, \dots, T_{pb}\}, \quad (4)$$

with $b = 1, 2, \dots, B$, and $B = 1000$

The FWER-adjusted p -value of the test, for each feature can be calculated as seen in “(5)”:

$$p\text{-value}_i = \frac{\sum_{b=1}^B I_{T_b^{JSD}} + 1}{B + 1}, \text{ with} \quad (5)$$

$$I_{T_b^{JSD}} = 1 \text{ if } T_b^{JSD} \geq T_i \text{ else } 0$$

For our experiments we consider a significance level of $\alpha = 5\%$ and focus on the Blackhole-Wormhole dilemma. Since $B = 1000$, $p = 7$, $k = 2$, we have the permutation test results in Tab. IV.

TABLE IV: Permutation Test Results

Feature	Jensen-Shannon Distance	p -value
LostPackets	0.376153	<0.001
RxBytes	0.743254	<0.001
RxByteRate/s	0.197168	1.000000
MeanDelay/s	0.546946	<0.001
MeanJitter/s	0.546824	<0.001
PacketDropRate	0.825746	<0.001
AverageHopCount	0.539645	<0.001

From Tab. IV we have p -value < α for all features, except “RxByteRate/s”, which leads us to reject H_0 for those features, meaning that their estimated KDEs are different at a significance level of $\alpha = 5\%$, but does not guarantee lack of overlap, of individual points. In the figures below, we present a few of the estimated densities, for each class, on the left and the p -values of the test, on the right. In order to analyze the misclassifications we must look at Fig. 16, where we can see clearly, the two densities of feature “PacketDropRate”. We notice the bimodal-density for the Wormhole category, where the smaller peak, seems to mimic the behavior of Blackhole attacks, in the overlap zone $[0.25, 1.4]$. High overlap percentage, in certain areas, share also the variables “MeanJitter/s”, “MeanDelay/s” and “AverageHopCount”. The phenomenon of Density Support Intersection, the overlap in the plots, is the one that confuses XGBoost, in so many features, due to absence of linear separability, even when the estimated densities seem statistically different, in terms of shape, with the Max-Statistic of Jensen-Shannon. The problem with this dataset is that even the best feature for distinguishing Blackhole from Wormhole attacks has a percentage of density overlap.

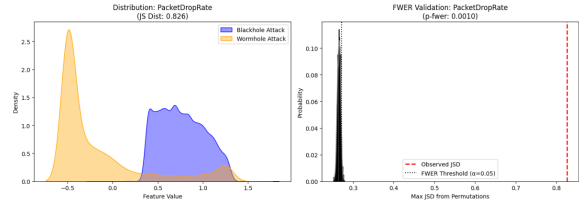


Fig. 16: Feature: PacketDropRate

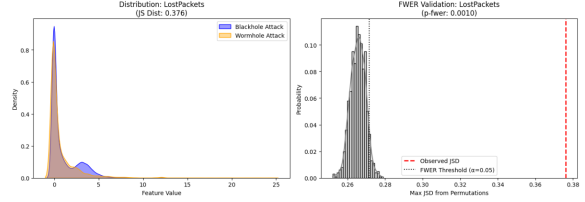


Fig. 17: Feature: LostPackets

IV. CONCLUSIONS

In this paper we applied best practices for data pre-processing and provided top-performing algorithms and hybrid models, that are capable to detect intrusions in UAV systems, compared to baseline models. After the selection of our best model, we move to SHAP analysis, where we establish solid proof of our model’s internal decision mechanisms, with local and global explanations, that help us clarify, which variables contribute to the predictions of the general tendency and which to individual data-points, per class. We didn’t simply describe the general idea, but gave specific examples of true and false predictions. With the visual density and shape analysis we analyzed and explained our data’s skewed, multi-modal densities and the false predictions that occur, due to the Support Intersection between Blackhole and Wormhole attacks. With the combination of the Westfall-Young test, the KDE and the JSD, we distinguish the different nature of the attacks, even with the high percentage of density overlap. These are proof that XGBoost’s false predictions, do not happen, because

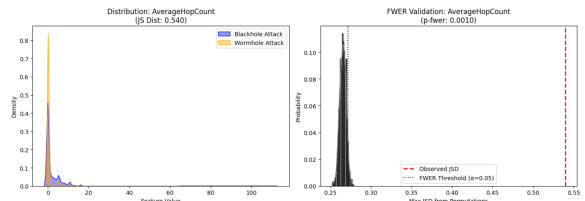


Fig. 18: Feature: AverageHopCount

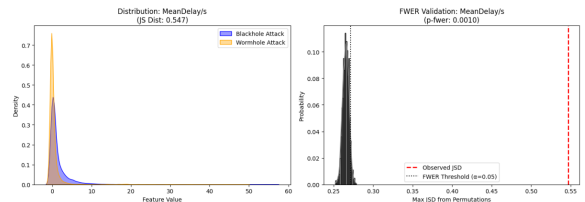


Fig. 19: Feature: MeanDelay/s

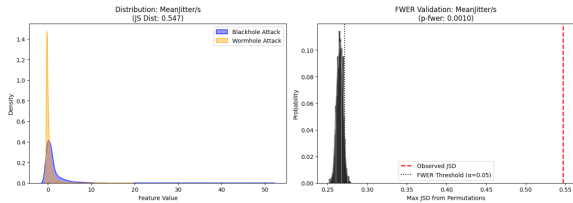


Fig. 20: Feature: MeanJitter/s

of weak training or data pre-processing, but because of the massive support intersection, in UAVIDS-2025. Even with this major problem our best model has an outstanding performance. By combining all the above techniques, we have a solid view of the attacks. Future work includes cross-dataset validation, with other well-known UAVIDS datasets, that share the same feature space, use of Deep-CNNs with 2D Convolutions for intrusion detection to capture the spatial characteristics and RNNs to handle the dataset as online training. Last but not least more XAI methods can be used for local and global explanations, like LIME, or gradient-based methods.

REFERENCES

- [1] A. A. Halimaa, K. Sundarakantham, “Machine Learning Based Intrusion Detection System”, IEEE International Conference on Trends in Electronics and Informatics, October, 2019, pp. 916-920, doi: 10.1109/ICOEI.2019.8862784.
- [2] A. Jamalipour, S. Murali, “A Taxonomy of Machine-Learning-Based Intrusion Detection Systems for the Internet of Things: A Survey”, IEEE Internet of Things Journal, vol. 9, no. 12, November, 2021, pp.9444-9466, doi: 10.1109/JIOT.2021.3126811.
- [3] C. B. Şahin, “Securing UAV Swarms with Vision Transformers: A Byzantine-Robust Federated Learning Framework for Cross-Modal Intrusion Detection”, Drones, vol.10, no.2, February, doi: 2026https://doi.org/10.3390/drones10020125.
- [4] D. Holzmüller, L. Grinsztajn, I. Steinwart, “Better by default: Strong Pre-Tuned MLPs and Boosted Trees on Tabular Data”, NeurIPS, 2024.
- [5] E. Haque, K. Hasan, I. Ahmed, M. S. Alam and T. Islam, “Towards an Interpretable AI Framework for Advanced Classification of Unmanned Aerial Vehicles (UAVs)”, IEEE 21st Consumer Communications and Networking Conference (CCNC), Las Vegas, NV, USA, 2024, pp. 644-645, doi: 10.1109/CCNC51664.2024.10454862.
- [6] I. Bibers, O. Arreche, W. Alayed, M. Abdallah, “Ensemble-IDS: An Ensemble Learning Framework for Enhancing AI-Based Network Intrusion Detection Tasks”, Applied Sciences, vo. 15, no. 19, September, 2025, doi: https://doi.org/10.3390/app151910579.
- [7] J. Romano, M. Wolf, “Exact and Approximate Stepdown Methods for Multiple Hypothesis Testing”, SSRN Electronic Journal, February, 2005, doi: 10.2139/ssrn.563267
- [8] L. K. Hansen, L. Rieger, “Interpretability in Intelligent Systems — A New Concept?”, Springer, September, 2019, pp. 41–49, doi: https://doi.org/10.1007/978-3-030-28954-6.
- [9] L. Lin, H. Ge, Y. Zhou, R. Shanguan, “UAV Airborne Network Intrusion Detection Method Based on Improved Stratified Sampling and Ensemble Learning”, Drones, vol. 9, no. 9, August, 2025, https://doi.org/10.3390/drones9090604.
- [10] K. P. Murphy, “Probabilistic Machine Learning: Advanced Topics”, Cambridge, Massachusetts, USA, MIT Press, 2023, pp.55-236.
- [11] M. A. Hossain, W. Ishtiaq, and M. S. Islam, “A Comparative Analysis of Ensemble-Based Machine Learning Approaches With Explainable AI for Multi-Class Intrusion Detection in Drone Networks”, Security and Privacy, vol. 9, no. 1, December, 2025, doi: https://doi.org/10.1002/spy2.70164.
- [12] M. Islam, F. Ahmed, W. Ishtiaq, M. Hossai, M. Tarek, “Advanced explainable ensemble models for multi-class intrusion detection in heterogeneous drone and industrial networks”, Journal of Information Security, Springer, March, 2026, doi: https://doi.org/10.1186/s13635-026-00234-w.
- [13] M. S. Islam, A. S. Mahmoud, T. R. Sheltami, “AI-Enhanced Intrusion Detection for UAV Systems: A Taxonomy and Comparative Review”, Drones, 2025, vol. 9, no. 10, doi: https://doi.org/10.3390/drones9100682.
- [14] M. Sarhan, S. Layeghy, M. Portmann, “An Explainable Machine Learning-Based Network Intrusion Detection System for Enabling Generalisability in Securing IoT Networks”, arXiv, April, 2021, doi: https://doi.org/10.48550/arXiv.2104.07183.
- [15] N. Erickson, J. Mueller, A. Shirkov, H. Zhang, P. Larroy, M. Li, A. Smola, “AutoGluon-Tabular: Robust and Accurate AutoML for Structured Data”, arXiv, March, 2020, doi: https://doi.org/10.48550/arXiv.2003.06505.
- [16] N. Meinshausen, M. H. Maathuis, P. Bühlmann, “Asymptotic optimality of the Westfall–Young permutation procedure for multiple testing under dependence”, The Annals of Statistics, vol. 39, no. 6, December, 2011, pp. 3369–3391, doi: 10.1214/11-AOS946.
- [17] P. H. Westfall, S. S. Young, “Resampling-Based Multiple Testing: Examples and Methods for p-Value Adjustment”, The Annals of Statistics, vol. 43, no. 2, June, 1994, pp. 347–348, doi: https://doi.org/10.2307/2348369
- [18] Q. Zeng, A. Bashir and F. Nait-Abdesselam, “UAVIDS-2025: A Benchmark Dataset for Intrusion Detection in UAV Networks Using Machine Learning Techniques”, 2025 IEEE Conference on Communications and Network Security (CNS), Avignon, France, 2025, pp. 1-9, doi: 10.1109/CNS66487.2025.11194990.
- [19] S. A. H. Mohsan, N. Q. H. Othman, Y. Li, M. H. Alsharif, and M. A. Khan, “Unmanned aerial vehicles (UAVs): practical aspects, applications, open challenges, security issues, and future trends”, Intelligent Service Robotics, vol. 16, no. 1, 2023, pp. 109–137, doi: 10.1007/s11370-022-00452-4.
- [20] S. Ergün, “Explaining XgBoost Predictions with SHAP Value: A Comprehensive Guide to Interpreting Decision Tree-Based Models”, New Trends in Computer Sciences, vol.1, no.1, April, 2023, pp. 19–31, doi: https://doi.org/10.3846/ntcs.2023.17901.
- [21] S. Kim, S. A. Kim, G. Kim, E. Menadjiev, C. Lee, S. Chung, N. Kim, J. Choi, “PnPXAI: A Universal XAI Framework Providing Automatic Explanations Across Diverse Modalities and Models”, arXiv, May, 2025, doi: https://doi.org/10.48550/arXiv.2505.10515.
- [22] S. M. Lundberg, S. L. Lee, “A Unified Approach to Interpreting Model Predictions”, NeurIPS, December, 2017, pp. 4765–4774, doi: https://doi.org/10.48550/arXiv.1705.07874.
- [23] S. Neupane, J. Ables, W. Anderson, S. Mittal, S. Rahimi, I. Banicescu and M. Seale, “Explainable Intrusion Detection Systems (X-IDS): A Survey of Current Methods, Challenges, and Opportunities”, IEEE Access, vol.10, no.7, January, 2022, doi: https://doi.org/10.48550/arXiv.2207.06236.
- [24] S. Niyonsaba, K. Konate and M. M. Soidridine, “Deep Learning Based Intrusion Detection for Cybersecurity in Unmanned Aerial Vehicles Network”, International Conference on Electrical, Computer and Energy Technologies (ICECET), Sydney, Australia, 2024, pp. 1-6, doi: 10.1109/ICECET61485.2024.10698453.
- [25] S. Wang, Z. Deng, FL. Chung, W. Hu, “From Gaussian kernel density estimation to kernel methods”. International Journal of Machine Learning and Cybernetics, vol. 4, no. 2, April, 2013, pp.119-37, doi: https://doi.org/10.1007/s13042-012-0078-8.
- [26] T. Yamaguchi, Y. Zhou, M. Ryo, K. Katsura, “Agentic Explainable Artificial Intelligence (Agentic XAI) Approach To Explore Better Explanation”, arXiv, December, 2025, doi: https://doi.org/10.48550/arXiv.2512.21066.
- [27] V. Arya, R. K. E. Bellamy, P.-Y. Chen, A. Dhurandhar, M. Hind, S. C. Hoffman, S. Houde, Q. V. Liao, R. Luss, A. Mojsilović, S. Mourad, P. Pedemonte, R. Raghavendra, J. Richards, P. Sattigeri, K. Shanmugam, M. Singh, K. R. Varshney, D. Wei, Y. Zhang, “One explanation Does Not Fit All: A Toolkit and Taxonomy of AI Explainability Techniques” arXiv, September, 2019, doi: https://doi.org/10.48550/arXiv.1909.03012.
- [28] V. U. Ihekoronye, S. O. Ajakwe, J. M. Lee and D.-S. Kim, “DroneGuard: An Explainable and Efficient Machine Learning Framework for Intrusion Detection in Drone Networks”, IEEE Internet of Things Journal, vol. 12, no. 7, pp. 7708-7722, April, 2025, doi: 10.1109/JIOT.2024.3519633.
- [29] Y.-W. Hong, D.-Y. Yoo, “Multiple Intrusion Detection Using Shapley Additive Explanations and a Heterogeneous Ensemble Model in an Unmanned Aerial Vehicle’s Controller Area Network”, Applied Sciences, vol. 14, no. 13, June, 2024, doi: https://doi.org/10.3390/app14135487.